Transverse Energy in Nucleus-Nucleus Collisions, A Review

Mark Tincknell
Oak Ridge National Laboratory

CONF-8810264--2

DE89 005131

November 15, 1988

Abstract

The status of Transverse Energy (E_T) in relativistic nucleus–nucleus collisions at the Brookhaven AGS and the CERN SPS is reviewed. The definition of E_T and its physical significance are discussed. The basic techniques and limitations of the experimental measurements are presented. The acceptances of the major experiments to be discussed are shown, along with remarks about their idiosyncrasies. The data demonstrate that the nuclear geometry of colliding spheres primarily determines the shapes of the observed spectra. Careful account of the acceptances is crucial to comparing and interpreting results. It is concluded that nuclear stopping power is high, and that the amount of energy deposited into the interaction volume is increasing with beam energy even at SPS energies. The energy densities believed to be obtained at the SPS are close to the critical values predicted for the onset of a quark-gluon plasma.

1 What is E_T ?

Transverse energy (E_T) is defined as the sum of the energies of particles weighted by the sine of their angle to the beam,

$$E_T = \sum_{i=1}^{N} E_i \sin\theta_i. \tag{1}$$

This energy is usually measured by calorimeters, which respond differently to different kinds of particles. For photons, calorimeters measure total energy. For mesons, they measure total relativistic energy, *i.e.* kinetic energy plus rest mass. Calorimetric energy for nucleons is just kinetic energy without rest mass, and for antinucleons it is kinetic energy plus twice the rest mass, due to annihilation. Formula (1) above may be rewritten as

$$E_T = \sum_{i=1}^{N} |p_{T,i}|(\sqrt{1+(m_i/p_i)^2} + q_i) \tag{2}$$

$$\text{where: } q_i = \begin{cases} 0 & \text{for mesons and photons,} \\ -m_i/p_i & \text{for nucleons,} \\ +m_i/p_i & \text{for antinucleons;} \end{cases}$$

thus:

$$E_T \approx \sum_{i=1}^{N} |p_{T,i}| \tag{3}$$

$$\text{for: } p_i = |\mathbf{p}_i| \gg m_i.$$

For particle momenta large compared to their rest masses, E_T is approximately the sum of the magnitudes of the transverse momenta, and is almost a Lorentz invariant. This is a good approximation for forward particles from fixed-target experiments with beam momenta above a few AGeV/cper nucleon.

Also note that

$$E_T = \sum_{i=1}^{N} m_{T,i}(\sqrt{1-(m_i \cos\theta_i/m_{T,i})^2} + q_i') \tag{4}$$

$$\text{where: } m_{T,i} = \sqrt{m_i^2 + p_{T,i}^2},$$

$$\text{and: } q_i' = \begin{cases} 0 & \text{for mesons and photons,} \\ -m_i \sin\theta_i/m_{T,i} & \text{for nucleons,} \\ +m_i \sin\theta_i/m_{T,i} & \text{for antinucleons;} \end{cases}$$

thus:

$$E_T \approx \sum_{i=1}^{N} m_{T,i} \tag{5}$$

$$\text{for: } m_{T,i} \gg m_i.$$

(The quantity m_T is useful for Lorentz transformation calculations involving rapidity, and for empirically scaling particle spectra to compare particles of different mass.)

2 Why is E_T interesting?

E_T is a global feature of all hadronic collisions. It is a direct measure of the violence of an interaction, and an indication of how much of the beam particle's energy has been harnessed for interesting processes. E_T is relatively easy to measure experimentally. Even though modern calorimeters are massive and and have hundreds or even thousands of readout channels, they are one of the few kinds of detectors that is affordable for covering large solid angles. Furthermore, E_T can be used as a selective trigger. The signals from calorimeters are often fast enough to be incorporated into online logic to decide whether to write an event to tape. Triggering on large E_T can enrich the data sample in interesting events. One may also use E_T in offline analysis to characterize the violence of events in correlation with other observables.

It is interesting to ask how projectile energy is degraded in hadronic collisions, and what happens to the energy lost by the projectile. This "nuclear stopping power" determines the amount of energy that can be deposited in the reaction zone, and how much passes transparently through it. Models of stopping power depend on the number and kind of interactions between the projectile and successive nucleons in the target, and on the basic properties of the hadronic collisions[1]. E_T is one of the simplest observables related to these fundamental processes.

E_T is produced by redirecting part of the longitudinal energy of the beam into an interaction. If the number of degrees of freedom and the space-time dimensions of the system are large enough, the interacting particles can scatter multiple times and approach thermalization. Thus, when concepts from statistical mechanics may be applied, E_T is an extensive observable of an (at least partially) thermalized system.

E_T may also serve as an indicator of the energy density achieved in high-energy collisions. Various theoretical treatments of hadronic interactions with relativistic hydrodynamic models show a direct proportionality between E_T and energy density[2]. Since energy density is directly related to expectations of a phase transition to a quark-gluon plasma, it is extremely important to deduce it from experimental results. Currently available models allow only crude estimates of energy density to be made from the observed E_Ts.

3 How is E_T measured?

E_T is almost always measured with calorimeters, although in principle, E_T could be calculated (approximately) from any data that contain the three-momenta of the particles emitted in a reaction. Calorimeters measure energy directed at various angles from the interaction point. They usually consist of a sandwich of many layers of absorber materials alternating with active layers to read out the energy; however some calorimeters, such as Pb-glass and NaI, are homogeneous. Both electromagnetic (photons, electrons, and positrons) and hadronic particles interact multiple times in the absorbing layers, creating showers of secondary particles that propagate into the calorimeter. In homogenous calorimeters, showers are formed and detected in the same medium[3].

Energy from electromagnetic particles may be experimentally distinguished from that of hadronic particles. Since the radiation length of an absorber can be much less than its hadronic interaction length, calorimeters are usually built with a front section that has a short effective radiation length, to absorb the EM energy, and a much longer rear section to contain the hadronic showers. Unfortunately, some hadronic interactions will occur in the EM section, and there can be leakage of EM energy into the hadron section. This can be corrected on average, but not perfectly for individual events.

Note that since hadronic collisions produce mostly pions, and roughly 1/3 of the pions are π^0s which decay predominantly into 2γ, about 1/3 of E_T is electromagnetic energy.

The energy signal is derived from the dE/dx energy loss deposited in the active layers along the paths of all the showering secondaries. Both the showering and the sampling processes are subject to large statistical fluctuations, particularly for hadronic showers. Thus, even for a perfectly calibrated calorimeter, the energies detected are only correct in an average sense, and the real energy may differ from the detected energy by as much as 1–2 times the calorimeter energy resolution. The energy resolution of a hadronic calorimeter is typically $\sigma/E \geq 0.3/\sqrt{E}$ for E measured in GeV.

The particle showers have a significant lateral spread. Because of the large multiplicity of energetic particles emanating at small angles to the beam from a relativistic nuclear collision, the showers usually overlap there, and individual particle energies cannot be distinguished. The lateral extent of the showers also shifts energy transversely. There is usually a strong gradient in the energy distribution of particles across the face of a calorimeter, and the lateral spread of shower energy will tend to diminish the observed gradient. This makes E_T in the raw data larger than the real value. Spreading effects can also be corrected on a statistical basis as long as the gradient is not large compared to the readout cell size.

In most experiments, the calorimeters cover only part of the total solid angle. At current experimental energies, the differential distribution of E_T as a function of pseudorapidity (angle) is peaked about mid-pseudorapidity. Thus E_T spectra measured by one group may differ significantly from those of another for the same beam, target, and energy, but different angular coverage. In particular, it is almost useless to compare the "maximum E_T" between experiments. Another crucial consequence of limited acceptance is that shifts in the angular distribution of E_T into and out of the experimental acceptance can cause variations in the observed E_T larger than actual changes in the E_T production. This point will be emphasized in the following discussion of the data.

A final remark about calorimetry is that the whole principle of measuring shower energy starts to break down for particles with energies $\lesssim 2$ GeV. In this regime, the calorimeter linearity, efficiency, and resolution all vary strongly as a function of particle energy and type. The shower and sampling statistical fluctuations become substantial compared to the energy measured. This is important for slow particles (*i.e.* near target rapidity) in fixed-target experiments, and for the central rapidity region in future RHIC experiments.

In summary, calorimeters are not simple black boxes that detect the energy of each emitted particle. Many of the experimental difficulties encountered with relativistic nuclear collisions cannot be properly evaluated with a test beam, and must be corrected with the help of Monte Carlo simulations. Because calorimeter data are usually averaged over many events, systematic uncertainties usually dominate over statistical errors in E_T spectra. In most E_T spectra, a $\pm 10\%$ (or more)

systematic error in the E_T scale is quite possible, even if it is not explicitly stated.

4 The Acceptances of the Major Experiments

This paper will discuss data from five major experiments: E802 and E814 at the Brookhaven AGS, and NA34, NA35, and WA80 at the CERN SPS. The angular coverage of the calorimetry of each one is quite different, and in the cases of E802, NA34, and NA35, the coverage has changed between runs.

Because the kinematic variable, rapidity,

$$y = \tanh^{-1}(\beta \cos\theta) \tag{6}$$

is approximately equal to the convenient angular variable, pseudorapidity,

$$\eta = \ln(\cot(\theta/2)) \tag{7}$$

$$\text{when: } \beta \approx 1,$$

the angular acceptances, and many later results, will be reported in η. At the AGS, there have been runs at 10.0 AGeV/c and 14.5 AGeV/c, corresponding to beam rapidities of 3.06 and 3.42 respectively. At the SPS, beam momenta of 60 AGeV/c and 200 AGeV/c have been used, or 4.84 and 6.06 in rapidity units. The nucleon-nucleon center-of-mass rapidity is simply 1/2 the beam rapidity, which can be used as a landmark for the forward-backward coverage of calorimeters in pseudorapidity units. Consult Figure 1 for an overview of the E_T acceptances of the five major experiments.

E802 at the AGS is primarily a spectrometer experiment, with a Pb-glass calorimeter for event characterization. In 1986, they ran with a preliminary configuration in which the Pb-glass modules were stacked in a rectangular wall covering approximately $1.2 < \eta < 2.4$, and 360° in azimuth. The Pb-glass did not contain hadronic showers, and could not distinguish the Čerenkov light contribution of hadrons from that of the EM showers. To estimate E_T, the total measured signal was multiplied by 0.5 to correct for the hadron Čerenkov component, multiplied by 3.0 to add the missing hadron energy to the observed EM energy, and multiplied by $< \sin\theta > = 0.29$ to account for the mean geometric factor[4]. This is a crude treatment that can provide a first glimpse of the E_T spectra, and will doubtlessly be improved in the future. In 1987, E802 restacked their Pb-glass into a semi-annular wall covering approximately $1.3 < \eta < 2.4$, and 180° in azimuth, with much better segmentation. Only preliminary data are available from that run.

E814 is a calorimeter and projectile fragmentation experiment at the AGS. In 1987 they ran an early configuration, using a wall of NaI crystals backed by a Uranium-Copper-scintillator calorimeter for hadronic energy. There was full 360° acceptance for approximately $1.7 < \eta < 3.1$, but the region $\eta > 2.5$ of the Uranium calorimeter is covered by four central modules that catch energy from projectile spectators (and beam particles) in addition to participants[5]. Only preliminary results are available from this experiment. In the near future, the final configuration of E814 will run with almost 4π calorimeter coverage. Future results from this collaboration will provide the best E_T data from nucleus-nucleus collisions at the AGS.

NA34 (Helios) is a very large experiment at the SPS that includes many diverse detector elements, including calorimeters. In 1986, they ran with Uranium-scintillator calorimeters covering $-0.1 < \eta < 2.9$, and 360° in azimuth. This region is mostly backward in the center-of-mass at SPS energies, and complements the other experiments that cover the c.m. and forward regions[6]. In the 1987 run, Helios upgraded their calorimetry to cover virtually 4π: $-0.1 < \eta < 5.5$, and 360°. This gives their calorimetry the best acceptance of any relativistic heavy ion experiment. Published data are available from the 1986 run, and there are some early results from 1987.

NA35 is a streamer chamber and calorimeter experiment at CERN. They measure E_T with a projective-readout EM calorimeter (the Photon Position Detector, PPD), and a 240-segment Pb-scintillator and Fe-scintillator Ring Calorimeter. The calorimeters have not changed between runs,

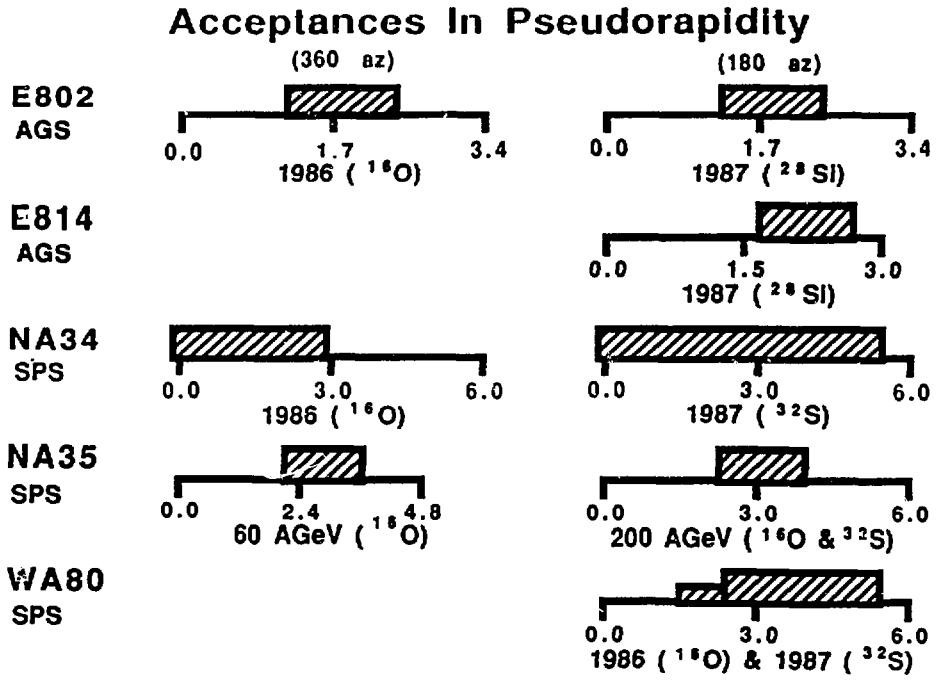

Figure 1: The E_T acceptances of the five experiments discussed in this paper, given in pseudorapidity units. The left and right columns represent different configurations of the same experiment. The horizontal scales are 0 to 3.4 units for the AGS experiments E802 and E814, and 0 to 6 units for the SPS experiments NA34 (Helios), NA35, and WA80. See the text for more details.

but the target–calorimeter distance was shifted between the 60 AGeV/c and 200 AGeV/c running to adjust the acceptance. For 60 AGeV/c, the Ring Calorimeter acceptance was roughly $2.1 < \eta < 3.7$, and for 200 AGeV/c, it was approximately $2.3 < \eta < 3.9$, all with full azimuthal coverage[7]. The projective nature of the PPD obscures some of the geometric information in the EM energy signal, which is reconstructed with the help of Monte Carlo simulations. Data from both 1986 and 1987 are available.

The final heavy ion experiment to be discussed is WA80 at the SPS. They have a rectangular wall of Pb-scintillator and Fe-scintillator calorimeter (the MId RApidity Calorimeter, MIRAC) covering 360° for approximately $2.4 < \eta < 5.5$, and partial azimuthal coverage (about 10%) between $1.6 < \eta < 2.4$. In addition, the Plastic Ball consists of 655 modules covering approximately $-1.7 < \eta < 1.3$, and 360°, and it can provide E_T data to complete much of the remaining solid angle[8]. Data from the 1986 run and preliminary data from 1987 are available from the MIRAC, but Plastic Ball results are still being analyzed.

5 Kinematics and Fireballs

Relativistic nuclear collisions are usually discussed in the participant-spectator picture, in which nuclei are (usually) spheres that collide with a definite impact parameter. The volumes of overlap participate in the reaction and are violently disrupted, while the remaining (spectator) volumes shear off and suffer comparatively mild excitation. The magnitude of E_T is determined by the bombarding energy, and by the participant volume (or equivalently, the number of participating nucleons). The cross section for a specific value of E_T depends on the geometric probability of a given impact parameter. For peripheral collisions, in this simple picture, the participating volumes are bounded by cylindrical cuts through the edges of the spheres. For near-central collisions of a light projectile with a heavy target, the whole projectile sphere and a cylindrical section from the target sphere participate. These simple considerations can explain all of the gross features of $d\sigma/dE_T$ spectra. The maximum number of participating nucleons for the case of $A_p \leq A_t$, in the idealization of sharp spheres colliding at zero impact parameter, is

$$\begin{aligned} N_p &= w_p/m_N = A_p, \text{ and} \\ N_t &= w_t/m_N = A_t - (A_t^{2/3} - A_p^{2/3})^{3/2}. \end{aligned} \tag{8}$$

(Here w_p (w_t) is the mass of the participating nucleons in the projectile (target), and m_N is the nucleon mass.)

The center-of-mass (c.m., more properly center-of-momentum) of the system is usually taken to be the c.m. of the participating volumes, and not $y_{beam}/2$, the nucleon-nucleon c.m. The c.m. rapidity is

$$y_{cm} = \tanh^{-1}\beta_{cm} = \tanh^{-1}\left(\frac{\beta_p}{1 + w_t/(\gamma_p w_p)}\right), \tag{9}$$

and the kinetic energy available in the participating system is

$$T_{cm} = \sqrt{w_p^2 + w_t^2 + 2\gamma_p w_p w_t} - (w_p^2 + w_t^2). \tag{10}$$

In principle, all this energy could be emitted at 90°, and that is the real *kinematic* limit for E_T. Of course, this does not occur in practice, and a more realistic limit is the case where this energy radiates isotropically, as if the participants stop in the c.m. and thermalize their available energy in a fireball. For isotropic emission,

$$E_T = \frac{1}{4\pi}\int T_{cm}\sin\theta\, d\Omega = \frac{\pi}{4}T_{cm}. \tag{11}$$

It can be shown that

$$\frac{dE_T}{dy} \approx \frac{<cp_T>N}{2}\mathrm{sech}^2(y - y_{cm}) \tag{12}$$

for an isotropic fireball radiating massless particles, and this distribution has a width $\Delta y(\mathrm{FWHM}) = 1.76$[9]. Observed is $\Delta\eta(\mathrm{FWHM}) \geq 2.6$ of $dE_T/d\eta$ for 200 AGeV/c ^{32}S projectiles at the SPS[10]. This suggests that there is longitudinal hydrodynamic expansion of the fireball that distributes E_T across a larger spread in y. Nevertheless, the isotropic fireball model is closer to the truth for AGS and SPS experiments than is the assumption that dE_T/dy is constant independent of y (*i.e.* boost invariant). That scenario may apply at *RHIC* energies (100 + 100 AGeV/c in the c.m.).

6 $d\sigma/dE_T$ is Determined by Nuclear Geometry!

A typical $d\sigma/dE_T$ spectrum from relativistic nuclear collisions of a light projectile and a heavy target has three distinct regions[11]. At low E_T, there is a high value of $d\sigma/dE_T$ (the "neck"), for intermediate E_T there is a broad "plateau" of constant or slowly dropping $d\sigma/dE_T$, and for large E_T, $d\sigma/dE_T$ falls off like the tail of a Gaussian distribution. The high value of $d\sigma/dE_T$ at low E_T comes from the large probability for a grazing collision of two spheres. The plateau region stems from the fact that participant volume grows more and more slowly with decreasing impact parameter, so broader and broader ranges of impact parameter produce similar E_T with roughly the same incremental probability. This occurs in the range where almost all of the light projectile is occluded by the larger target; the plateau is absent for collision partners of similar mass. The tail at high E_T occurs for collisions at nearly zero impact parameter (central collisions).

For central collisions, the participant volumes are very insensitive to impact parameter. The Gaussian form of the tail comes from fluctuations in the number of nucleon-nucleon scatters, due to the random distribution of the nucleons in the incoming nuclei. Such fluctuations are much more probable than the occurrence of "hard" parton-parton scatters. A factor that can affect the tail is the orientation of the axes of deformed nuclei at the time of collision. If one or both of the incident nuclei is not spherical, then the number of participating nucleons is significantly higher if the "fat" direction is aligned with the collision axis. Such fluctuations in orientation decrease the steepness of the tail[11].

Corroboration of the participant-spectator picture comes from the strong anticorrelation of E_T with the energy of the projectile spectators, as measured by a calorimeter at zero degrees (E_{ZDC} or E_{veto}). The smaller the impact parameter, the larger the participant volume and E_T, and the smaller the spectator volume and E_{veto}[7]. E_T also correlates tightly with produced particle multiplicity. This is due to the fact that hadronic interactions produce particles with very similar values of $|p_T|$, and so E_T and multiplicity are proportional by equation (3). The $d\sigma/dN$ spectra have virtually an identical shape to $d\sigma/dE_T$[18].

Intranuclear cascading has an important affect on E_T. Slow produced particles form inside the original nuclei, and can rescatter with spectator nucleons, multiplying the number of energetic particles. This can significantly increase in $dE_T/d\eta$ in the target pseudorapidity range, where angles are large and $\sin\theta$ has maximal weight. E_T is *not* a conserved quantity, and it can be affected by complicated reaction dynamics.

7 How Does E_T Scale with Participants?

Early analyses from NA35, and more detailed analyses from E802, have compared E_T production from p + A and ^{16}O+ A. NA35 fit the shoulder and high E_T tail of their 200 AGeV/c ^{16}O + Pb $d\sigma/dE_T$ spectra with a 16-fold convolution of "central" p + Au data[19]. They argued that the selection of p + Au events with small impact parameters was necessary for a valid comparison with the correlated impact parameters of the 16 Oxygen nucleons in central ^{16}O + Pb collisions. This analysis reproduced the high E_T part of the ^{16}O + Pb spectrum quite well.

E802 has done a much more comprehensive analysis, fitting the entire shape of the $d\sigma/dE_T$ spectra of 14.5 AGeV/c ^{16}O + Cu, and ^{16}O+ Au, from p + Au data averaged over all impact parameters[20]. They used two (numerical) parameters to fit the p + Au $d\sigma/dE_T$ spectrum with a gamma distribution. They employed a Glauber-type Monte Carlo model to predict the probability of n ($\leq$ 16) ^{16}O nucleons interacting in the target, and produced the n-fold convolution of the p + Au gamma distribution. Adding these contributions for $n = 1$ to $n = 16$, weighted by the Glauber probabilities, they obtained very good fits to both the ^{16}O + Cu and ^{16}O + Au $d\sigma/dE_T$ spectra for all values of E_T. This may be called the Wounded *Projectile* Nucleon (WPN) model. See Figure 2.

WA80 has presented an interesting alternative analysis of their data. They used the projectile spectator energy in their Zero Degree Calorimeter (ZDC), and the help of the Fritiof Monte Carlo model, to derive the number of target and projectile participant nucleons on an event-by-event basis[8,17]. They have shown that E_T per participant is almost constant at a given bombarding energy (either 60 AGeV or 200 AGeV), for every projectile (^{16}O and ^{32}S), target (C, Al, Cu, Ag, and Au), and ZDC energy (impact parameter). This is the basis of several of the interpretations presented in other sections. It is a straightforward extension of the Wounded Nucleon (WN) model from p + A physics[21,22]. See Figure 2.

The WPN model and WN model are not consistent with each other, and neither is free from questions of internal consistency either. The WPN fits from E802 used p + Au data without impact parameter selection, yet the impact parameters of the ^{16}O nucleons are obviously correlated for individual events. The agreement between p + *Au* convolutions and ^{16}O + *Cu* spectra is also surprising. These data suggest that nuclear thickness has little to do with E_T production at AGS energies: the first one or two nucleon-nucleon collisions determine the E_T originating from each projectile nucleon. This idea supports the overall picture of complete energy-stopping at the AGS. It is important to note that the $d\sigma/dN$ spectra from E802 are well fit by a WN model. This discrepancy has been attributed to the effect of slow protons, which contribute to the multiplicity count, but scale disproportionately to the π^0 multiplicity, and cannot themselves be observed by a Čerenkov signal in the Pb-glass calorimeters[12].

At SPS energies, the WN model describes a lot of p + A data. The physical picture depends on Lorentz time dilation and the time-energy uncertainty relation to delay the formation of produced particles beyond the dimensions of the original nuclei (longitudinal growth). This allows nucleons to collide multiple times while traversing a nucleus, but incur little or no additional excitation, and produce little secondary cascading. Yet, it is a puzzle why E_T per participant should be the same for peripheral collisions and the nucleons at the front of the colliding nuclei, and for nucleons at the rear of the colliding nuclei. The nucleons at the rear should be colliding with nucleons that have already lost energy, and so should produce E_T like interactions at lower beam energy. The WA80 data do show a factor of ~ 2 difference between E_T per participant at 60 AGeV/c and 200 AGeV/c (the same factor as the ratio of c.m. energies). It is reasonable to propose that ^{16}O is such a small nucleus that there is no "rear", and thus explain NA35's good fit with the convolved proton $d\sigma/dE_T$ spectra. The WA80 results are harder to understand, unless the slowing is relatively small and the effect cannot be observed within the errors in their data. A conjecture is that slowing is closely related to particle production, and so energy loss is negligible for all nucleon-nucleon collisions before the formation time of the secondary particles.

8 How Does E_T Scale with A_t?

One of the important claims that has been made is that there is "complete" stopping in medium and heavy targets at AGS energies[20]. This is supported by the observation that the high E_T tails of the $d\sigma/dE_T$ spectra start to coincide as the target mass increases. For both ^{16}O and ^{28}Si projectiles bombarding targets of ^{27}Al, ^{nat}Cu (mass 64), ^{nat}Ag (mass 108), and ^{197}Au, the tails approach an apparent maximum E_T value in the progression from Cu to Au. See Figure 3. The particle multiplicity spectra $d\sigma/dN$ have a very similar shape (and physical relationship because of

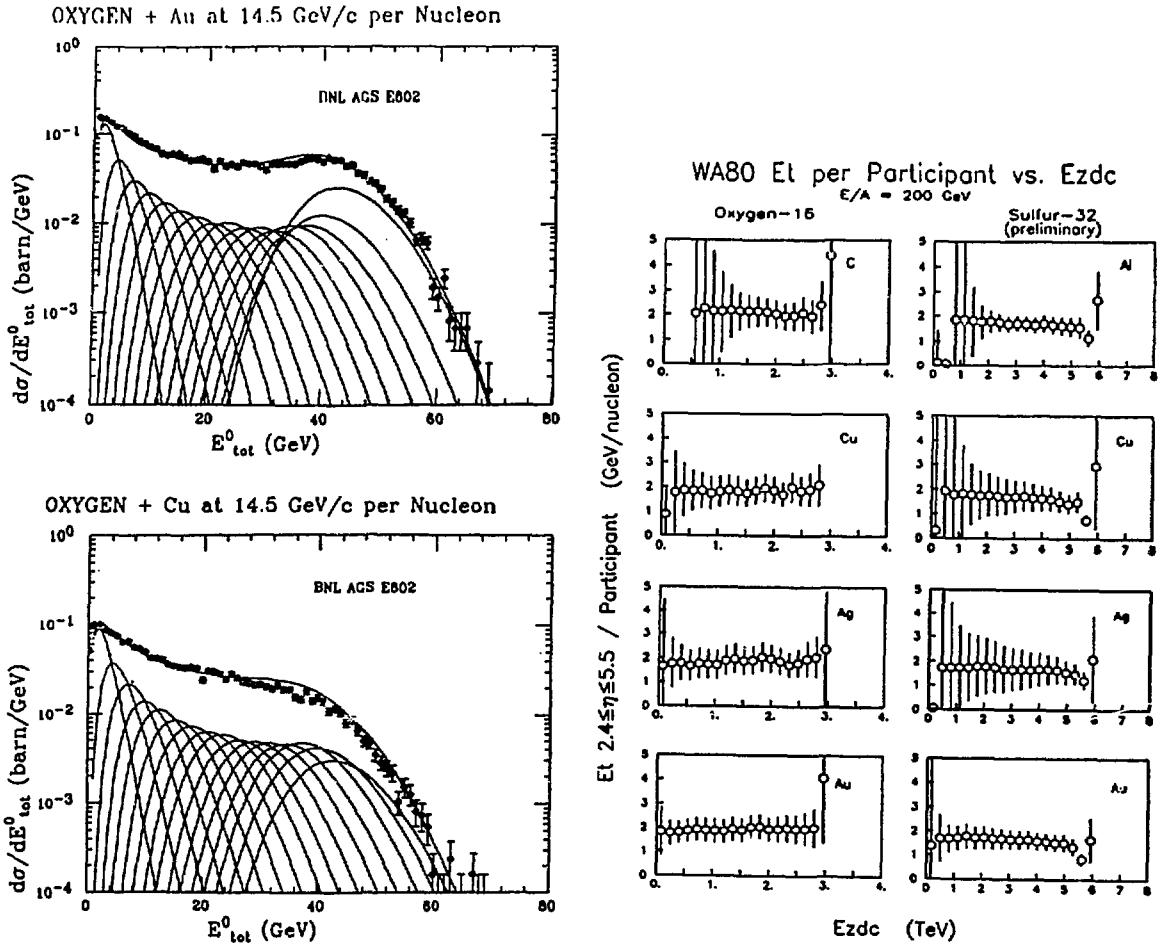

Figure 2: On the left are data from E802 at the AGS, for ^{16}O + Cu and ^{16}O + Au at 14.5 *A*GeV/*c*. These $d\sigma/dE^0$ *vs.* E^0 spectra are well reproduced by a 1- to 16-fold convolution of the inclusive p + Au spectrum, weighted by Glauber probabilities (see text). (E^0 is the observed Čerenkov signal in their Pb-glass calorimeter; $E^0 \propto E_T$.) This implies that E_T spectra at AGS energies are determined by the number of wounded *projectile* nucleons.

On the right are data from WA80 at the SPS, for ^{16}O + C, Cu, Ag, Au, and ^{32}S + Al, Cu, Ag, and Au, all at 200 *A*GeV/*c*. Plotted is E_T per participant nucleon as a function of *projectile* spectator energy in their Zero Degree Calorimeter (E_{ZDC}). The number of participants was determined from the E_{ZDC} with the help of the Fritiof Monte Carlo code. The data show that E_T is independent of projectile, target, and centrality (E_{ZDC}), and depends only on the total number of wounded nucleons and the beam energy.

equation (3)), except that the high multiplicity tails do not bunch together with increasing target mass. This could be interpreted as saturation in the energy deposition of the projectile: above a certain target mass, the whole projectile energy is shared by more and more target nucleons, but E_T does not increase.

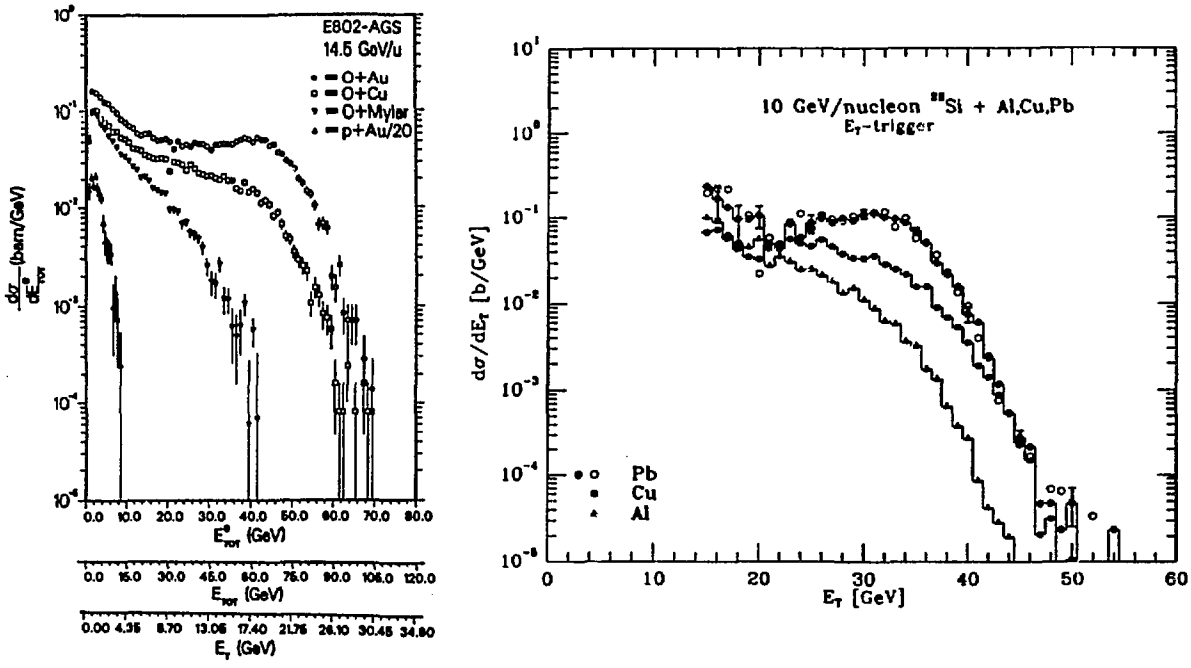

Figure 3: On the left are $d\sigma/dE^0$ spectra from E802 at the AGS. (E^0 is the observed Čerenkov signal in the E802 Pb-glass calorimeter.) The data are for p + Au, ^{16}O + Mylar, Cu, and Au at 14.5 AGeV/c. The alternate abscissas E^0_{TOT} and E_T are simply assumed to be proportional to E^0. Note the convergence of the high E^0 tails of the ^{16}O + Cu and ^{16}O + Au spectra, which has been interpreted as "complete stopping."
On the right are $d\sigma/dE_T$ spectra for ^{28}Si + Al, Cu, and Pb at 10.0 AGeV/c from E814 at the AGS. Again the high E_T tails of the Cu and Pb target distributions converge, suggesting that a maximum energy deposition as a function of target mass is already reached by the Cu target (mass 64). This cannot be decided definitively until results are available with more complete angular coverage.

However, a note of caution is in order. Both calorimeter setups run at the AGS to date (E802 in 1986 and 1987, and E814 in 1987) have had only partial pseudorapidity coverage. The $dE_T/d\eta$ distributions are peaked about $\eta_{cm}(\approx y_{cm})$, and y_{cm} shifts further backward from the nucleon-nucleon c.m. with increasing target mass and increasing collision centrality. This can shift an important part of $dE_T/d\eta$ out of the calorimeter acceptance, and mimic the effect of complete stopping. The "fireball" y_{cm} for ^{16}O + Au at 10 AGeV/c is 1.03, and the (preliminary) E814 coverage was complete (*i.e.* 360°) only for $\eta > 1.7$. The backward limit of the η coverage of E802 was $\eta \gtrsim 1.3$, while the fireball c.m. rapidity is 1.21 for 14.5 AGeV/c. Complete stopping may well be true at AGS energies, but convincing confirmation of it must await future data from the more complete angular coverage of E814.

At SPS energies, stopping appears to be less than 100%. Including Helios data from $-0.1 < \eta < 2.9$ for ^{16}O + W at 200 AGeV/c[6], and WA80 data covering $2.4 < \eta < 5.5$ for 200 AGeV/c ^{16}O + Au[8], the total E_T (for $d\sigma/dE_T$ at the "shoulder": the high E_T edge of the plateau, just

before the tail) can be estimated to be $\sim$ 210 GeV. The total available c.m. energy for the 16 + 52 nucleon system at 200 AGeV/c is 530 GeV, and the isotropic fireball E_T would be 420 GeV. Thus the observed E_T is $\sim 210/420 = 50\%$ of the fireball maximum. An estimate using the Landau hydrodynamic model, which incorporates longitudinal expansion more realistically than the isotropic fireball, finds that the fraction of stopped energy varies between 76% and 84% for ^{16}O + Cu and ^{16}O + Au at 200 AGeV/c[13].

NA35 has studied the functional dependence of E_T on A_t for 200 AGeV/c ^{16}O on various targets. They examined the scaling of E_T at the point on the tail of $d\sigma/dE_T$ where the cross section is down to 1% of the plateau value. The data fit a $\sim A_t^{0.29}$ power law[14]. The 1% point selects very central collisions, in which all 16 Oxygen nucleons participate, so E_T scaling should be determined by the variation in the (larger) number of target participants. The geometric model predicts that the target participant volume for central collisions is cylindrical, with radius of the ^{16}O projectile, and length of the target diameter. Thus E_T should scale with the target radius, $\sim A_t^{1/3}$, very close to what is observed. A later analysis by NA35 claimed a $A_t^{0.2}$ dependence, and contrasted this with the $A_t^{0.5}$ scaling seen by Helios in a more backward pseudorapidity range[7]. These results illustrate that the functional dependence of E_T on various parameters is strongly affected by the experimental acceptance and the method used to extract the parameterization.

Recent data from NA35 taken with ^{32}S beams at 200 AGeV/c on five targets show a steady increase in the E_T value at the shoulder of the $d\sigma/dE_T$ spectra[15]. When the E_T axes of these spectra are scaled by the $E_{T,max}$ of the isotropic fireball for each colliding system the spectra bunch together. However, the shoulder E_Ts of the scaled distributions do increase with increasing target mass, advancing from $E_T/E_{T,max} \approx 0.22$ for S + S, to ≈ 0.30 for S + Au. This demonstrates that stopping is still increasing with target mass at the highest SPS energies. See Figure 4.

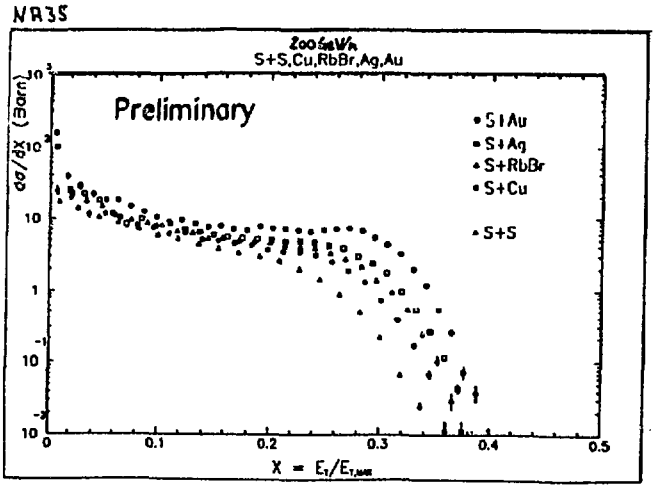

Figure 4: Data from NA35 at the SPS for ^{32}S + S, Cu, RbBr, Ag, and Au at 200 AGeV/c. The $d\sigma/dE_T$ spectra have been scaled by $E_{T,max}$ of the isotropic fireball calculated individually for the central collision limit of each of the five systems. The $X = E_T/E_{T,max}$ at the high E_T shoulder of the $d\sigma/dX$ spectra increases with target mass, demonstrating that relatively more E_T is produced with heavier targets at SPS energies. This implies that stopping is less than 100%.

9 How Does E_T Scale with A_p?

There are no AGS data on E_T scaling with A_p, because no experiment has yet run there with different nuclear beams and the same calorimeter setup. At the SPS, the geometric model suggests that the variation of the cylindrical volume of the target participants dominates the scaling of E_T with A_p. Since the cylinder radius varies as $\sim A_p^{2/3}$, this model predicts the ratio of E_T for ^{32}S to that for ^{16}O should be $(32/16)^{2/3} \approx 1.59$. Another argument, including the contribution from the number of *projectile* participants growing as A_p^1, predicts $A_p^{5/6}$ scaling[16].

At the Quark Matter '88 Conference, both NA35[15] and WA80[17] showed new E_T spectra overlaying ^{32}S + Au and ^{16}O + Au data at 200 AGeV/c, in which the E_T scale for ^{16}O was multiplied by a factor to adjust the high E_T tail to overlap with the ^{32}S data. The factor was 1.77 for NA35, and 1.60 for WA80. See Figure 5. These factors agree well with the geometric value, and the difference between the two may again be an artifact of acceptance. The NA35 Ring calorimeter covers $2.3 < \eta < 3.9$, which straddles mid-pseudorapidity, while WA80 spans the whole forward hemisphere with $2.4 < \eta < 5.5$. As will be discussed below, most of the variation of E_T occurs in the peak of $dE_T/d\eta$, about $\eta_{cm} \pm 1$. NA35 covers only (part of) this region, while WA80 covers the same range, plus forward angles where E_T does not vary as significantly. Thus the difference WA80 sees in E_T production between ^{16}O and ^{32}S may be diluted compared to NA35's observation, because of WA80's additional forward coverage.

Unfortunately, $dE_T/d\eta$ spectra from NA35 and WA80 are not yet available to show just where in pseudorapidity the additional E_T from the ^{32}S projectile arises. An important hint is offered by recent data from Helios, which reported first results from their complete calorimetry, covering $-0.1 < \eta < 5.5$. For the reaction ^{32}S + W at 200 AGeV/c, they have presented $dE_T/d\eta$ plots, for four different event classes based on total E_T[10]. See Figure 6. For the (relatively) low total E_T class, the distribution is broad and roughly symmetric about $\eta = 3.0$ (the nucleon-nucleon c.m.), appropriate for peripheral collisions. Progressing to the higher total E_T classes, a prominent peak develops at $\eta \approx 2.5$ (the central ^{32}S + W fireball c.m.), and there is very little, if any, increase in E_T above $\eta > 4.0$. Since E_T scales up with total participant number at the SPS, almost independent of beam and target, it is plausible to suggest that this behavior occurs for ^{16}O + Au as well, and explains why NA35 and WA80 find different scaling exponents for E_T as a function of A_p.

The $\Delta\eta$(FWHM) of the four $dE_T/d\eta$ distributions *decreases* with increasing total E_T. Crudely measured, it is $\Delta\eta$(FWHM) ≈ 3.8 for the lowest $137.6 < E_T < 160.6$ GeV class, and drops to $\Delta\eta$(FWHM) ≈ 2.6 for the highest $436 < E_T < 459$ GeV class. This suggests an increasing fireball character in the events with higher total E_T.

10 What Can Be Learned About Energy Densities?

Although the energy density threshold for the transition to a quark-gluon plasma (QGP) is not accurately predicted by current theories, many sources concur that the critical value is in the range 2–4 GeV/fm^3[23]. At present, there is not a reliable and well-established way to measure the energy density (ε) experimentally. WA80 has tried to estimate it from their E_T data, with the help of existing (albeit simplistic) theoretical models. In their first attempt, they failed to account for the diminished participant volume at low E_T, and so they underestimated ε for non-central events[24]. Recently, they have used two different theoretical formulations to calculate ε on an event-by-event basis, for arbitrary impact parameters[17].

The first model is the oft-quoted Bjorken formula[2],

$$\varepsilon_{BJ} = \frac{(dE_T/dy)|_{cm}}{F c\tau_0}, \tag{13}$$

where $(dE_T/dy)|_{cm} (\approx (dE_T/d\eta)|_{cm})$ is the peak transverse energy per unit rapidity, F is the face area of the participating sections of the nuclei, and $c\tau_0$ is the proper formation length, canonically

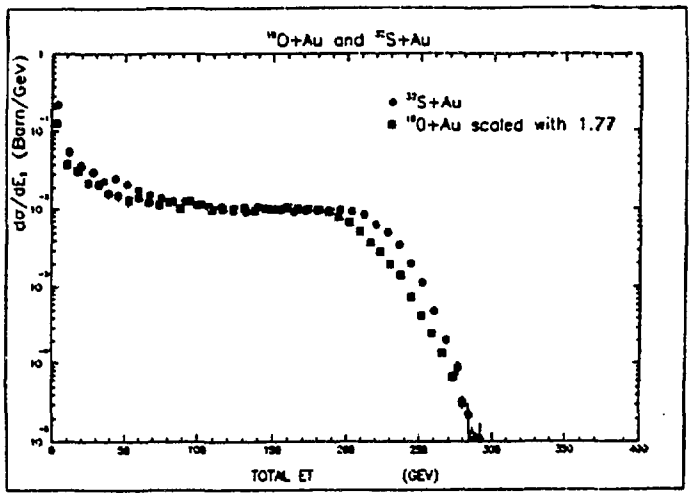

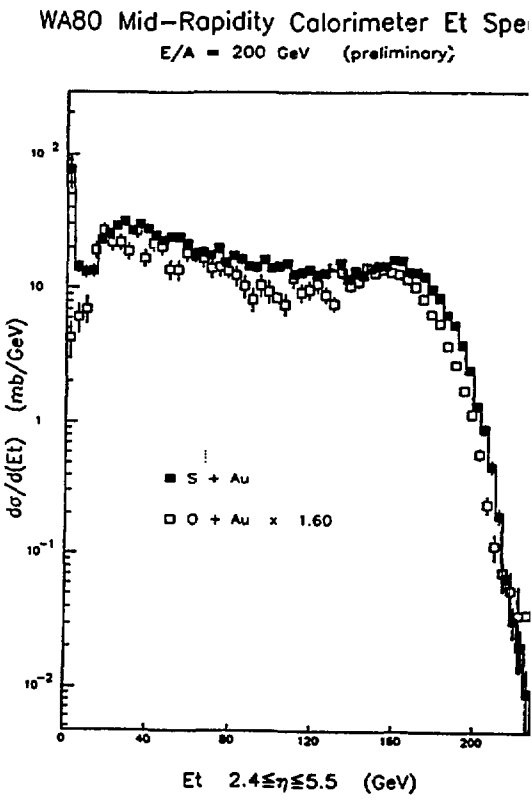

Figure 5: On the left, data from NA35 at the SPS for ^{16}O + Au and ^{32}S + Au at 200 AGeV/c. The E_T scale for the ^{16}O spectrum is multiplied by 1.77 to approximately align the high E_T tails of the distributions.
On the right, ^{16}O + Au and ^{32}S + Au $d\sigma/dE_T$ spectra at 200 AGeV/c from the WA80 Collaboration. In this case, the factor on the ^{16}O E_T scale is 1.60. The difference between the NA35 and the WA80 factors demonstrates the effect of acceptance on parameters extracted from E_T spectra.

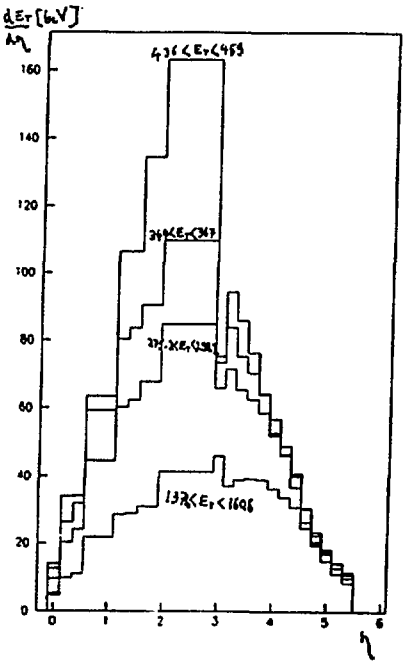

Figure 6: A preliminary $dE_T/d\eta$ *vs.* η plot from Helios for the system ^{32}S + W at 200 AGeV/c. The four distributions are for different event classes based on total E_T (going from the lowest peak $dE_T/d\eta$ to the highest): $137.6 < E_T < 160.6, 275.2 < E_T < 298.2, 344 < E_T < 367$, and $436 < E_T < 459$ GeV. Note that the $dE_T/d\eta$ values converge for all four classes for $\eta > 4.0$, indicating that E_T in that pseudorapidity range depends little on the number of participants. Also note that the $\Delta\eta$(FWHM) decreases significantly between the lowest and highest total E_T classes, perhaps indicating an increasing fireball character with increasing centrality.

taken to be 1 fm. For central collisions of a light projectile with a heavy target, the face area is taken to be $F = \pi(r_0 A_p^{1/3})^2$, but this can be generalized to any impact parameter. In the geometric model, the face area is either the circular area of the projectile disk for complete "dive-in", or the lenticular area of intersection of the projectile and target disks for more peripheral collisions. See the face area F depicted in the transverse view in Figure 7. Bjorken derived the formula under the assumption that there is a flat plateau in dE_T/dy as a function of rapidity y, which is a poor approximation for energies as low as the SPS experiments. It may be true at RHIC energies.

The questionable applicability of Bjorken's formula to the present data has stirred a search for alternative formulations. One such alternative is the fireball model, in which the energy density is merely the fireball energy divided by the fireball volume,

$$\varepsilon_{FB} = E_{FB}/V_{FB}. \tag{14}$$

For an isotropic fireball, the total energy is simply proportional to the total transverse energy via equation (11). The missing angular coverage of the WA80 calorimeters may be roughly corrected by assuming

$$E_{FB} = \frac{4}{\pi} E_T(\text{Total}) \approx \frac{8}{\pi} \int_{\eta_{cm}}^{\infty} \frac{dE_T}{d\eta} d\eta. \tag{15}$$

The fireball volume may be estimated from the cylinder taken at a time in the c.m. frame just after the rear edges of the nuclei have finished passing through each other. The volume of the cylinder is the product of the face area of the participants, and a length equal to the sum of the Lorentz-contracted diameters of the participating sections plus a 1 fm formation length for the produced particles to materialize after the collisions of the rear-most nucleons. See Figure 7 for an illustration of the dimensions of this volume. This formula[25],

$$V_{FB} = F\left(\frac{<D_p>}{\gamma_{p,cm}} + \frac{<D_t>}{\gamma_{t,cm}} + c\tau_0\right), \tag{16}$$

lessens the dependence of ε_{FB} on the unknown parameter $c\tau_0$, compared with Bjorken's denominator. As with the face area F, the mean diameters $<D>$ and Lorentz γ_{cm} factors may be generalized to non-zero impact parameters.

As defined above, both ε_{BJ} and ε_{FB} can be calculated for each event from the observed $dE_T/d\eta \approx dE_T/dy$ distribution, and from the impact parameter of the collision which is deduced from the ZDC energy with the help of the Fritiof model[17].

WA80 has presented ε spectra for three colliding systems: ^{16}O + Au at 60 AGeV/c, ^{16}O + Au at 200 AGeV/c, and ^{32}S + Au at 200 AGeV/c[17]. These data show that the Bjorken energy density is indeed in the range of 1–3 GeV/fm^3. The fireball model estimates of energy density are in the range 1–4 GeV/fm^3, even higher than Bjorken's estimates. See Figure 8. The most probable energy densities increase significantly going from 60 AGeV/c to 200 AGeV/c, but the increase in going from ^{16}O to ^{32}S at 200 AGeV/c is small. The increase in going from 60 AGeV/c to 200 AGeV/c is a factor of ~ 2, corresponding directly to the difference in c.m. energy. It is interesting to note that ε is much less correlated with impact parameter than E_T is. This behavior implies that energy density does not depend strongly on the number of participants, but merely on the colliding energy. Increasing the participants does increase the volume and time over which the fireball may equilibrate, and possibly, the chances of forming the QGP.

It may be hoped that more refined theoretical models, applicable to the current experimental energies, will be available in the near future, and that they will give much more precise estimates of energy density from E_T.

11 What Has Been Learned from E_T?

In this article, the following major points have been emphasized:

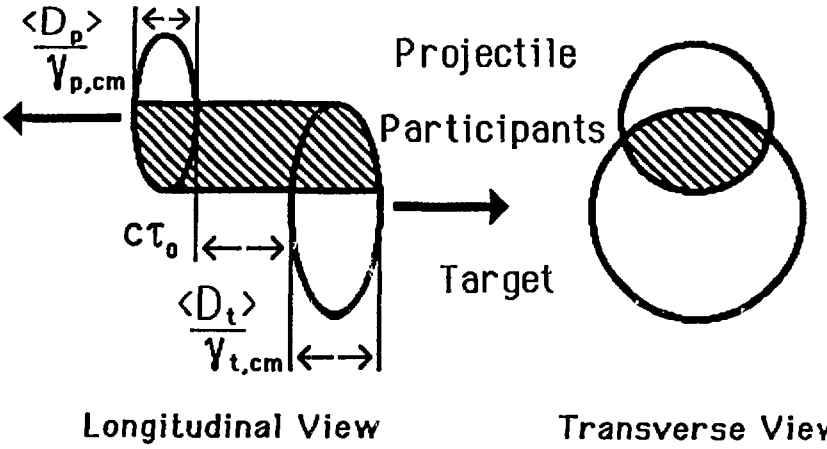

Figure 7: A schematic representation of the volume used by WA80 to calculate energy density (ε) in the fireball model. On the left is a longitudinal view depicting the three terms contributing to the length of the participant volume, and on the right is the transverse view, showing the face area used for non-central collisions. The volume is *length* × *area*. The effect of Lorentz contraction on the longitudinal thicknesses of the nuclei has been reduced from that at 200 AGeV/c for clarity.

- the nuclear geometry of colliding spheres, and the distinction of collision participants and spectators, are fundamental in explaining $d\sigma/dE_T$;
- there is no "plateau" in $dE_T/d\eta$ at current experimental energies, and account of the limited experimental acceptances is crucial to interpreting quantitative E_T results;
- "nuclear stopping power" may be almost complete at AGS energies, and it is still high at SPS energies;
- E_T seems to proportional to the number of projectile participant nucleons at AGS energies, but it is determined by the total number of participants at SPS energies;
- simple models allow estimates of energy density, which is found to be near the predicted critical value for the onset of the phase transition to the quark-gluon plasma;
- small gains can be made in energy density by increasing projectile mass, and potentially large increases in energy density are available by increasing c.m. energy.

12 Acknowledgements

The author expresses his appreciation to M. Tannenbaum and the E802 Collaboration, P. Braun-Munzinger and the E814 Collaboration, J. Schukraft and the Helios (NA34) Collaboration, J. Harris and the NA35 Collaboration, S. Sorensen and the WA80 Collaboration, R. Ledoux, F. Plasil, and J. Rafelski, for use of their preliminary data, analyses, and wisdom.

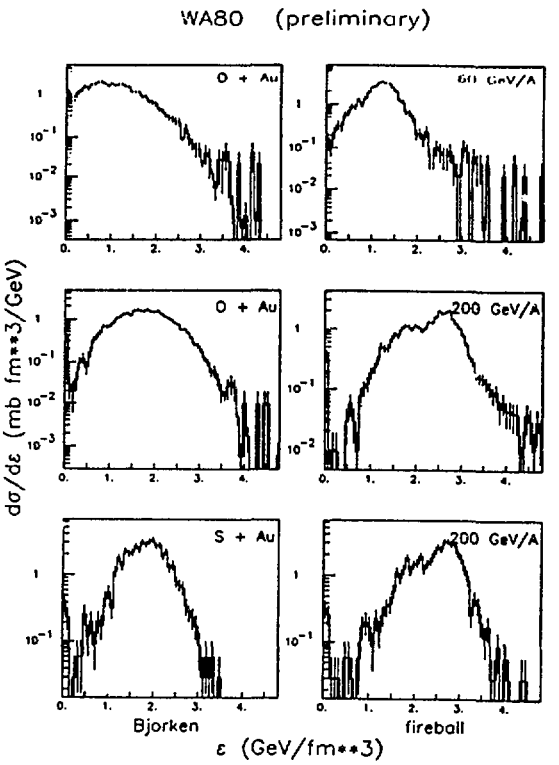

Figure 8: Energy density spectra obtained by WA80 for (from top to bottom): ^{16}O + Au at 60 AGeV/c, ^{16}O + Au at 200 AGeV/c, and ^{32}S + Au at 200 AGeV/c. On the left are the results from the Bjorken formulation, equation (13), and on the right are energy densities determined by the fireball model, equations (14), (15), and (16). See text for more details. Note that the energy densities obtained are similar in both models, and that ε varies much more strongly for the increase in beam energy from 60 AGeV/c to 200 AGeV/c than it does for the increase in projectile mass from ^{16}O to ^{32}S.

References

[1] Cheuk-Yin Wong, Phys. Rev. **C33**, 1340 (1986).

[2] J.D. Bjorken, Phys. Rev. **D27**, 140 (1983).

[3] C.W. Fabjan, T. Ludlam, Ann. Rev. Nuc. Part. Sci. **32**, 335 (1982).

[4] L.P. Remsberg and M.J. Tannenbaum, *et al.*, E802 Collaboration, Z. Phys. **C38**, 35 (1988).

[5] P. Braun-Munzinger, *et al.*, E814 Collaboration, Z. Phys. **C38**, 45 (1988).

[6] F. Corriveau, *et al.*, HELIOS Collaboration, Z. Phys. **C38**, 15 (1988).

[7] W. Heck, *et al.*, NA35 Collaboration, Z. Phys. **C38**, 19 (1988).

[8] S.P. Sorensen, *et al.*, WA80 Collaboration, Z. Phys. **C38**, 3 (1988).

[9] J. Rafelski, private communication.

[10] J. Schukraft, *et al.*, HELIOS Collaboration, Proceedings of the Seventh International Conference on Ultra-Relativistic Nucleus-Nucleus Collisions, Quark Matter 1988, Lennox, Mass., U.S.A., to be published in Nuc. Phys. **A**, 1989.

[11] J. Schukraft, "Review of E_T and Multiplicity Distributions in Heavy-Ion Collisions," preprint CERN-EP/88-141, also Proceedings of the 19th Symposium on Multiparticle Dynamics, Arles, France (1988).

[12] Michael J. Tannenbaum, "Collisions at 14.5 GeV per Nucleon: The Study of Baryon-Rich Matter at High Energy," preprint BNL-41608, also Nucleus-Nucleus Collisions III, Proceedings of the Third International Conference on Nucleus-Nucleus Collisions, St. Malo, France, North-Holland–Amsterdam, pp. 555-584c, (1988).

[13] J. Stachel and P. Braun-Munzinger, "Stopping in High Energy Nucleus-Nucleus Collisions: Analysis in the Landau Hydrodynamic Model," submitted to Phys. Lett. **B**, Aug. 1988.

[14] R. Stock, *et al.*, NA35 Collaboration, "Investigation of Oxygen Induced Reactions at 200 GeV per Nucleon," Proceedings of the International Workshop on Gross Properties of Nuclei and Nuclear Excitations XV, Hirschegg, Austria, 1987.

[15] J. Harris, *et al.*, NA35 Collaboration, Proceedings of the Seventh International Conference on Ultra-Relativistic Nucleus-Nucleus Collisions, Quark Matter 1988, Lennox, Mass., U.S.A., to be published in Nuc. Phys. **A**, 1989.

[16] P. Braun-Munzinger, Proceedings of the Seventh International Conference on Ultra-Relativistic Nucleus-Nucleus Collisions, Quark Matter 1988, Lennox, Mass., U.S.A., to be published in Nuc. Phys. **A**, 1989.

[17] G.R. Young, *et al.*, WA80 Collaboration, Proceedings of the Seventh International Conference on Ultra-Relativistic Nucleus-Nucleus Collisions, Quark Matter 1988, Lennox, Mass., U.S.A., to be published in Nuc. Phys. **A**, 1989.

[18] I. Lund, *et al.*, WA80 Collaboration, Z. Phys. **C38**, 51 (1988).

[19] NA35 Collaboration, A. Bamberger, *et al.*, Phys. Lett. **B184**, 271 (1987).

[20] E-802 Collaboration, T. Abbott, *et al.*, Phys. Lett. **B197**, 285 (1987).

[21] P.M. Fishbane and J.S. Trefil, Phys. Rev. **D9**, 168 (1974); Phys. Lett. **B51**, 139 (1974).

[22] K. Gottfried, Phys. Rev. Lett. **32**, 957 (1974).

[23] H. Satz, Ann. Rev. Nucl. Part. Sci. **35**, 245 (1985).

[24] WA80 Collaboration, R. Albrecht, *et al.*, Phys. Lett. **B199**, 297 (1987).

[25] WA80 Collaboration, T.C. Awes, *et al.*, "Energy Measurements in Oxygen-Induced Reactions at 60 *A*GeV and 200 *A*GeV," Proceedings of the International Workshop on Gross Properties of Nuclei and Nuclear Excitations XVI, Hirschegg, Austria, 1988.

DISCLAIMER